
Study on Structural, Electronic, Optical and Mechanical Properties of MAX Phase Compounds and Applications

Review Article

Md. Atikur Rahman^{*}, Md. Zahidur Rahaman

Department of Physics, Pabna University of Science and Technology, Pabna-6600, Bangladesh

Email address:

atik0707phy@gmail.com (Md. Atikur Rahman)

To cite this article:

Md. Atikur Rahman, Md. Zahidur Rahaman. Study on Structural, Electronic, Optical and Mechanical Properties of MAX Phase Compounds and Applications Review Article. *American Journal of Modern Physics*. Vol. 4, No. 2, 2015, pp. 75-91. doi: 10.11648/j.ajmp.20150402.15

Abstract: The term “MAX phase” refers to a very interesting and important class of layered ternary transition-metal carbides and nitrides with a novel combination of both metal and ceramic-like properties that have made these materials highly regarded candidates for numerous technological and engineering applications. A relatively new class of transition metal layered compounds $M_{n+1}AX_n$ (MAX phases) where M is an early transition metal, A is a group A element most likely Al, and X is C or N with $n = 1, 2, 3, \dots$. Due to their unique structural arrangements and directional bonding, these ternary compounds possess some very outstanding mechanical and chemical properties such as damage-resistance, oxidation resistance, excellent thermal and electric conductivity, machinability, and fully reversible dislocation-based deformation. These properties can be explored in the search for new phases and their composites to meet the performance goals of advanced materials with applications in fossil energy conversion technology. Systematic and detailed computational studies on MAX phase compounds can provide fundamental understanding of the key characteristics that lead to these desirable properties and to the discovery of other new and better alloys. In this paper, we review on structural, electronic, optical and mechanical properties of around 50 MAX phase compounds and their applications. From the comparative study on the result of these compounds we think that this paper will enable to researcher to explore and predict new MAX phases and new composite alloys with better physical properties as advanced materials for various applications at extreme conditions.

Keywords: MAX Phase Compounds, Electronic, Optical and Mechanical Properties, Applications

1. Introduction

Metallic materials are typically characterized by being thermally and electrically conductive, plastically deformable at room temperature, readily machinable, thermal shock resistant, damage tolerant, relatively soft, etc. On the other hand, ceramics are generally characterized by high elastic moduli, good high temperature mechanical properties, good oxidation and corrosion resistance, etc. The relatively recent discovery of a family of new materials, namely the MAX phases [1] (also termed in some publications ‘metallic ceramics’ [2]) has provided materials that possess a useful combination of both metallic and ceramic characteristics. Recently, the interest in nanolaminated ternary $M_{n+1}AX_n$ (denoted 211, 312 and 413, where $n=1, 2$ and 3 , respectively) carbides and nitrides, so-called MAX-phases, has grown significantly. MAX phases are a family of ternary layered compounds with the formal stoichiometry $M_{n+1}AX_n$ ($n = 1, 2,$

$3, \dots$), where M is the transition d metal; A is the p element (e.g., Si, Ge, Al, S, Sn, etc.); X is carbon or nitrogen. Most of the MAX phases are 211 phases, some are 312s, and the rest are 413s. The M group elements include Ti, V, Cr, Zr, Nb, Mo, Hf, and Ta. The A elements include Al, Si, P, S, Ga, Ge, As, Cd, In, Sn, Tl, and Pb. The X elements are either C and/or N. First reports on the synthesis of MAX phases were presented in the works by Novotnoi et al. [3-7] performed in the 60’s of the last century. Intensive studies of the physicochemical properties of MAX phases, started in the middle of the 1990’s, led to the conclusion that they were a unique class of layered materials combining chemical, physical, electrical, and mechanical properties inherent to both metals and ceramics [8]. Thus, similarly to metals, MAX phases have good heat and electric conductivity and at the same time, like ceramics, they are refractory, oxidation and corrosion resistant and have low density. These properties can be explored in the search for new phases and their composites

that have potential to meet the performance goals for materials to be used in the next generation of fossil energy power systems at a significantly reduced cost. MAX phases are at present of increased interest as promising materials for polyfunctional high-temperature ceramics, protective coatings, sensors, and electrical contacts for catalysis. The current stage of the experimental studies of MAX phases is marked by the development of synthesis methods for these compounds, including in film and nanocrystalline states, and also by the discovery of new phases [9-11]. For example, by the magnetron deposition method new phases of Ti_4SiC_3 and

Ti_4GeC_3 (in the film state) along with a few others [11] have fairly recently been synthesized [12, 13]. Note that at present the family consists of 60 compounds [11] involving many d and p elements as components (Fig. 1). Moreover, detailed investigations of the functional properties of MAX phases (in particular, doping and non-stoichiometry effects, polymorphism, tribological, mechanical, and newly found [14, 15] superconducting properties, etc.) as well as further searches for the promising technological use of these materials are being conducted [11].

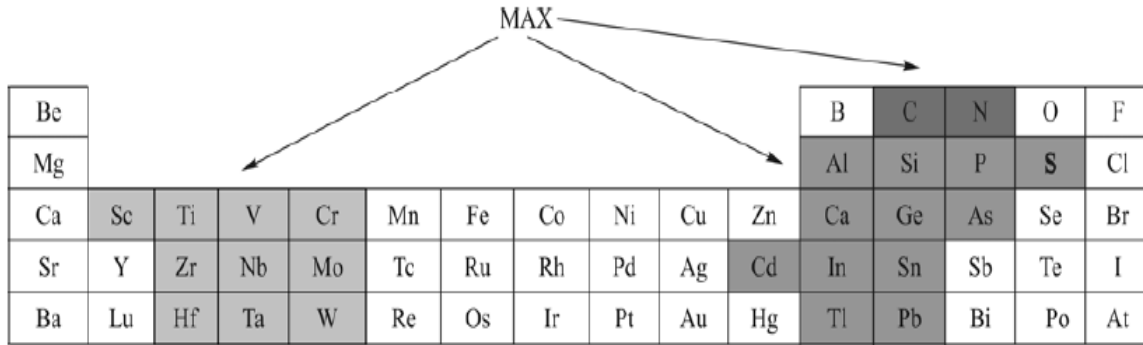


Fig. 1. Periodic table of elements forming nanolaminates of the general composition $M_{n+1}AX_n$ ($n = 1, 2, 3 \dots$), where M is a transition d metal, A is a p element (Si, Al, S, Sn, etc), and X is carbon or nitrogen.

There are more than 70 known phases of MAX compounds and this number is rapidly growing. A list of MAX phase compounds are shown in Table 1.

Table 1. A list of the MAX phases known to date, in both bulk and thin film form.

211 Phases	312 Phases	413 Phases
Ti_2CdC , Sc_2InC , Ti_2AlC , Ti_2GaC , Ti_2InC , Ti_2TiC , V_2AlC , Cr_2GaC , Ti_2AlN , Ti_2GaN , Ti_2InN , V_2GaC , V_2GaN , Cr_2GaN , Ti_2PbC , V_2GeC , Cr_2AlC , Cr_2GeC , Ti_2GeC , Ti_2SnC , V_2PC , Zr_2TiC , Nb_2AlC , Nb_2GaC , Nb_2InC , V_2AsC , Ti_2SC , Zr_2InC , Zr_2PbC , Nb_2SnC , Nb_2PC , Mo_2GaC , Zr_2InN , Zr_2TiN , Zr_2SnC , Nb_2AsC , Zr_2SC , Nb_2SC , Hf_2InC , Hf_2TiC , Ta_2AlC , Ta_2GaC , Hf_2SnC , Hf_2PbC , Hf_2SnN , Hf_2SC	Ti_3AlC_2 , V_3AlC_2 , Ti_3SiC_2 , Ti_3GeC_2 , Ti_3SnC_2 , Ta_3AlC_2	Ti_4AlN_3 , V_4AlC_3 , Ti_4GaC_3 , Ti_4SiC_3 , Ti_4GeC_3 , Nb_4AlC_3 , Ta_4AlC_3

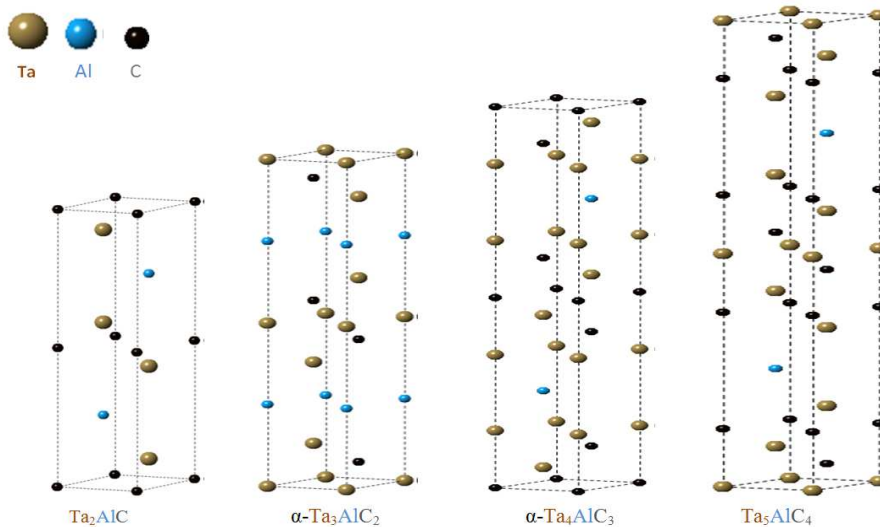


Fig. 2. Crystal structure of 211, 312, 413, 514 phases of $M=Ta$, $A=Al$ and $X=C$.

In this article, we review the electronic structure and mechanical properties of MAX phase compounds which have

been done using first-principles methods. Some of them are: Ti_3AC_2 ($A = Al, Si, Ge$), Ti_2AC ($A = Al, Ga, In, Si, Ge, Sn, P, As, S$), Ti_2AlN , M_2AlC ($M = V, Nb, Cr$), $Ta_{n+1}AlC_n$ ($n = 1$ to 4), Hf_2TiC , Hf_2SnC , Hf_2PbC , Hf_2SnN and Hf_2SC (see Table 1). Most of them are Ti-containing phases, since they are the most common in MAX phases. They are chosen for a wide representation and for studying specific trends. The first 12 vary only by the A element and involve three (3 1 2) phases and the nine (2 1 1) phases. In addition to carbides, one example of nitride, Ti_2AlN is also included. This is followed by three other (2 1 1) phases, $(V, Nb, Cr)_2AlC$ where the transition metal M have different d-electron configurations. The Ta-Al-C group is chosen to study the effect of the number of MX layers (see Fig.2). The calculated results include: band structures, total and partial density of states, effective atomic charges, quantitative bond order values, interband optical conductivities, elastic coefficients, bulk modulus, shear modulus, Young's modulus, and Poisson's ratio. By systematically analyzing these results and in comparison with available experimental data, several important features on structural stability, interatomic bonding and optical conductivities are identified. These results enable us to build a data base to facilitate the search for new MAX phases and new composite alloys with the potential of having better physical properties as advanced materials.

The publication of papers on the MAX phases has shown an almost exponential increase in the past decade. The existence of further MAX phases has been reported or proposed. In addition to surveying this activity, the synthesis of MAX phases in the forms of bulk, films and powders is reviewed, together with their physical, mechanical and corrosion/oxidation properties. Recent research and development has revealed potential for the practical application of the MAX phases (particularly using the pressureless sintering and physical vapour deposition coating routes) as well as of MAX based composites. The challenges for the immediate future are to explore further and characterize the MAX phases reported to date and to make further progress in facilitating their industrial application.

2. Early History of MAX Phase Compounds

The MAX phases have two histories. The first spans the time they were discovered in the early and mid-1960s to roughly the mid-1990s, when, for the most part, they were ignored. The second is that of the last 15 years or so, when interest in these phases has exploded. The ternary compound, Ti_3SiC_2 , was first synthesized and fully characterized by Dr. Michel Barsoum's research group at Drexel University in the 1990s. A year later they showed that this compound was but one of over sixty phases,[16] most discovered and produced in powder form in the 1960s by H. Nowotny and coworkers [17]. In 1999 they discovered Ti_4AlN_3 and realized that they were dealing with a much larger family of solids that all behaved similarly. Since 1996, when the first paper was

published on the subject, tremendous progress has been made in understanding the properties of these phases and the 1996 article [18] has been cited over 650 times [19].

3. Crystal Structures of MAX Phase Compounds

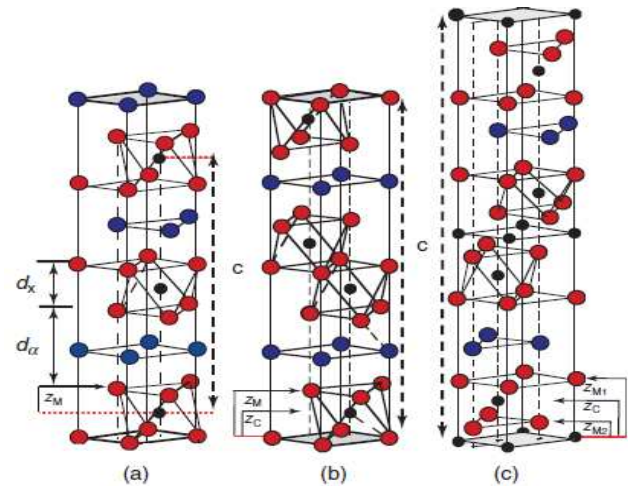


Fig. 2.1. Unit cells of (a) 211, (b) 312 and (c) 413 phases. The c parameters are depicted by vertical dashed lines. d_x denotes the thickness- from atom center to center of the $M_{n+1}X_n$ layers; d_α that of A layers. It follows that for the 211 phases $c = 2 d_\alpha + 2 d_x$. Also shown are the various z values (see Table 2).

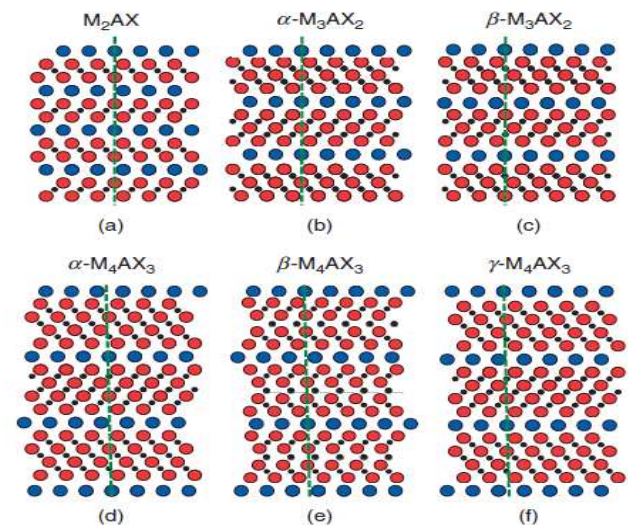


Fig. 3. Schematics of (1120) planes in (a) M_2AX , (b) α - M_3AX_2 , (c) β - M_3AX_2 , (d) α - M_4AX_3 , (e) β - M_4AX_3 and (f) γ - M_4AX_3 . Note that it is only in the α - M_3AX_2 structure that the A atoms lie on top of each other.

MAX-phase crystals have a hexagonal symmetry in space group $P63/mmc$. For the 211 structure, there are three inequivalent atoms; in the 312, there are four, and in the 413, there are five. The coordinates and internal parameters Z_M of all the atoms are listed in Table 2 for the various polymorphs. For the 211 phases, there is only one polymorph (Figure 3a). In the 312 case there are two, α and β , shown in Figures 3b and c, respectively. For the 413 phases, there are three

polymorphs, viz. α , β , and γ , shown in Figures 3d, e and f, respectively. The density (D) and lattice parameters (a, c) of MAX phase compounds are listed in Table 3 [22-35].

Table 2. Sites and idealized coordinates of the $M_{n+1}AX_n$ phases for $n = 1-3$. Also listed are the currently known polymorphs. The fifth column lists the canonical positions.

Atoms	Chemistry/archetypical phase				Z_M Range	Notes and reference
	M_2AX / Ti_2SC				-	Kudielka and Rohde (1960)
	Wyckoff	x	y	Z_i (canonical)	-	-
A	2d	1/3	2/3	$\frac{3}{4}$	-	-
M	4f	2/3	1/3	1/12 (0.083)	0.07-0.1	Z_M in Figure 2.1a
X	2a	0	0	0	-	-
	α - M_3AX_2/Ti_3SiC_2				-	Jeitschko and Nowotny (1967)
A	2b	0	0	4/16	-	-
M_I	4f	1/3	2/3	2/16 (0.125)	0.131- 0.138	Z_{M_I} in Figure 2.1b
M_{II}	2a	0	0	0	-	-
X_I	4f	2/3	1/3	1/16 (0.0625)	0.0722	Z_C in Figure 2.1b
	β - M_3AX_2/Ti_3SiC_2				-	Farber et al. (1999)
A	2d	1/3	2/3	4/16	-	Should be quite similar in
M_I	4f	1/3	2/3	2/16 (0.125)	0.1355	Properties to α - M_3AX_2
M_{II}	2a	0	0	0	-	-
X_I	4f	2/3	1/3	1/16 (0.0625)	0.072	-
	α - M_4AX_3/Ti_4AlN_3				-	Barsoum et al. (1999c) and Rawn et al. (2000)
A	2c	1/3	2/3	5/20	-	-
M_I	4e	0	0	3/20 (0.15)	0.155-0.158	Z_{M_I} in Figure 2.1c
M_{II}	4f	1/3	2/3	1/20 (0.05)	0.052-0.055	$Z_{M_{II}}$ in Figure 2.1c
X_I	2a	0	0	0	-	-
X_{II}	4f	2/3	1/3	2/20	0.103-0.109	Z_C in Figure 2.1c
	β - M_4AX_3/Ta_4AlC_3				-	Eklund et al. (2007)
A	2c	1/3	2/3	5/20	-	-
M_I	4e	1/3	2/3	12/20 (0.6)	0.658	-
M_{II}	4f	1/3	2/3	1/20	0.055	Eklund et al. (2007)
X_I	2a	0	0	0	-	-
X_{II}	4e	2/3	1/3	2/20	0.103	-
	γ - M_4AX_3/Ta_4GaC_3				-	Etzkorn et al. (2009)
A	2c	1/3	2/3	5/20	-	-
M_I	4e	0	0	3/20 (0.15)	0.156	-
M_{II}	4f	1/3	2/3	1/20	0.056	Etzkorn et al. (2009) and He et al. (2011)
X_I	2a	0	0	0	-	-
X_{II}	4f	2/3	1/3	2/20	0.1065	-

Table 3. Density and lattice parameters of 77 Max phase compounds.

No.	Compounds	Density D, (Mgm ⁻³)	Lattice parameters a, c(Å)
211 Phases			
1	Sc ₂ AlC	2.99	3.280, 15.373
2	Sc ₂ GaC	3.93	3.253, 15.813
3	Sc ₂ InC	4.72	3.272, 16.452
4	Sc ₂ TiC	6.60	3.281, 16.530
5	Ti ₂ AlC	4.11	3.051, 13.637
6	Ti ₂ AlN	4.31	2.989, 13.614
7	Ti ₂ SiC	4.35	3.052, 12.873
8	Ti ₂ PC	4.56	3.191, 11.457
9	Ti ₂ SC	4.62	3.216, 11.22
10	Ti ₂ GaC	5.53	3.07, 13.52
11	Ti ₂ GaN	5.75	3.00, 13.3
12	Ti ₂ GeC	5.30	3.07, 12.93
13	Ti ₂ AsC	5.71	3.209, 11.925
14	Ti ₂ CdC	9.71	3.1, 14.41
15	Ti ₂ InC	6.30	3.134, 14.077
16	Ti ₂ InN	6.54	3.07, 13.97
17	Ti ₂ SnC	6.10	3.163, 13.679
18	Ti ₂ TiC	8.63	3.15, 13.98
19	Ti ₂ PbC	8.55	3.20, 13.81

No.	Compounds	Density D, (Mgm ⁻³)	Lattice parameters a, c(Å)
20	V ₂ AlC	4.07	3.1, 13.83
21	V ₂ SiC	5.20	2.955, 11.983
22	V ₂ PC	5.38	3.077, 10.91
23	V ₂ GaC	6.39	2.93, 12.84
24	V ₂ GaN	5.94	3.00, 13.3
25	V ₂ GeC	6.49	3.00, 12.25
26	V ₂ AsC	6.63	3.11, 11.3
27	Cr ₂ AlC	5.21	2.863, 12.814
28	Cr ₂ GaC	6.81	2.88, 12.61
29	Cr ₂ GaN	6.82	2.875, 12.77
30	Cr ₂ GeC	6.88	2.95, 12.08
31	Zr ₂ AlC	5.78	3.2104, 14.2460
32	Zr ₂ AlN	5.83	3.2155, 14.2134
33	Zr ₂ SC	6.20	3.40, 12.13
34	Zr ₂ InC	7.1	3.34, 14.91
35	Zr ₂ InN	7.53	3.27, 14.83
36	Zr ₂ SnC	6.9	3.3576, 14.57
37	Zr ₂ TiC	9.17	3.36, 14.78
38	Zr ₂ TiN	9.60	3.3, 14.71
39	Zr ₂ PbC	8.2	3.38, 14.66
40	Nb ₂ AlC	6.50	3.10, 13.8
41	Nb ₂ PC	7.09	3.28, 11.5
42	Nb ₂ SC _{0.4}	7.01	3.27, 11.4
43	Nb ₂ SC _x	-	-
44	Nb ₂ GaC	7.73	3.13, 13.56
45	Nb ₂ InC	8.3	3.17, 14.37
46	Nb ₂ SnC	8.3	3.214, 13.802
47	Nb ₂ AsC	8.025	3.31, 11.9
48	Mo ₂ GaC	8.79	3.01, 13.18
49	Hf ₂ AlC	10.23	3.2121, 14.3830
50	Hf ₂ AlN	10.92	3.1380, 14.1872
51	Hf ₂ SC	11.36	3.36, 11.99
52	Hf ₂ InC	11.24	3.309, 14.723
53	Hf ₂ SnC	11.2	3.320, 14.388
54	Hf ₂ SnN	7.72	3.31, 14.3
55	Hf ₂ TiC	13.65	3.32, 14.62
56	Hf ₂ PbC	11.5	3.55, 14.46
57	Ta ₂ AlC	11.46	3.079, 13.860
58	Ta ₂ GaC	13.05	3.10, 13.57
312 Phases			
1	Ti ₃ SiC ₂	4.52	3.0665, 17.671
2	Ti ₃ AlC ₂	4.2	3.065, 18.487
3	Ti ₃ GeC ₂	5.22	3.07, 17.76
4	Ti ₃ SnC ₂	5.99	3.1366, 18.650
5	V ₃ SiC ₂	5.27	2.915, 17.535
6	(V _{0.5} Cr _{0.05}) ₃ AlC ₂	5.31	2.892, 17.73
7	Nb ₃ SiC ₂	7.22	3.13, 17.94
8	Ta ₃ AlC ₂	12.43	3.0930, 19.159
413 Phases			
1	Ti ₄ AlN ₃	4.58	2.988, 23.372
2	Ti ₄ SiC ₃	4.65	3.05, 22.67
3	Ti ₄ GeC ₃	-	-, 22.7
4	V ₄ AlC ₃	5.24	2.931, 22.719
5	Nb ₄ AlC ₃	6.97	3.123, 24.109
6	α-Nb ₄ SiC ₃	-	3.1819, 22.9877
7	Ta ₄ AlC ₃	13.18	3.092, 23.708
8	Ti ₄ GaC ₃	5.17	3.0690, 23.440
514 Phase			
1	Ti ₅ SiC ₄	4.81	3.04, 27.24
615 Phase			
1	Ta ₆ AlC ₅	13.69	3.078, 34.681
716 Phase			
1	Ti ₇ SnC ₆	4.80	3.2, 4.1

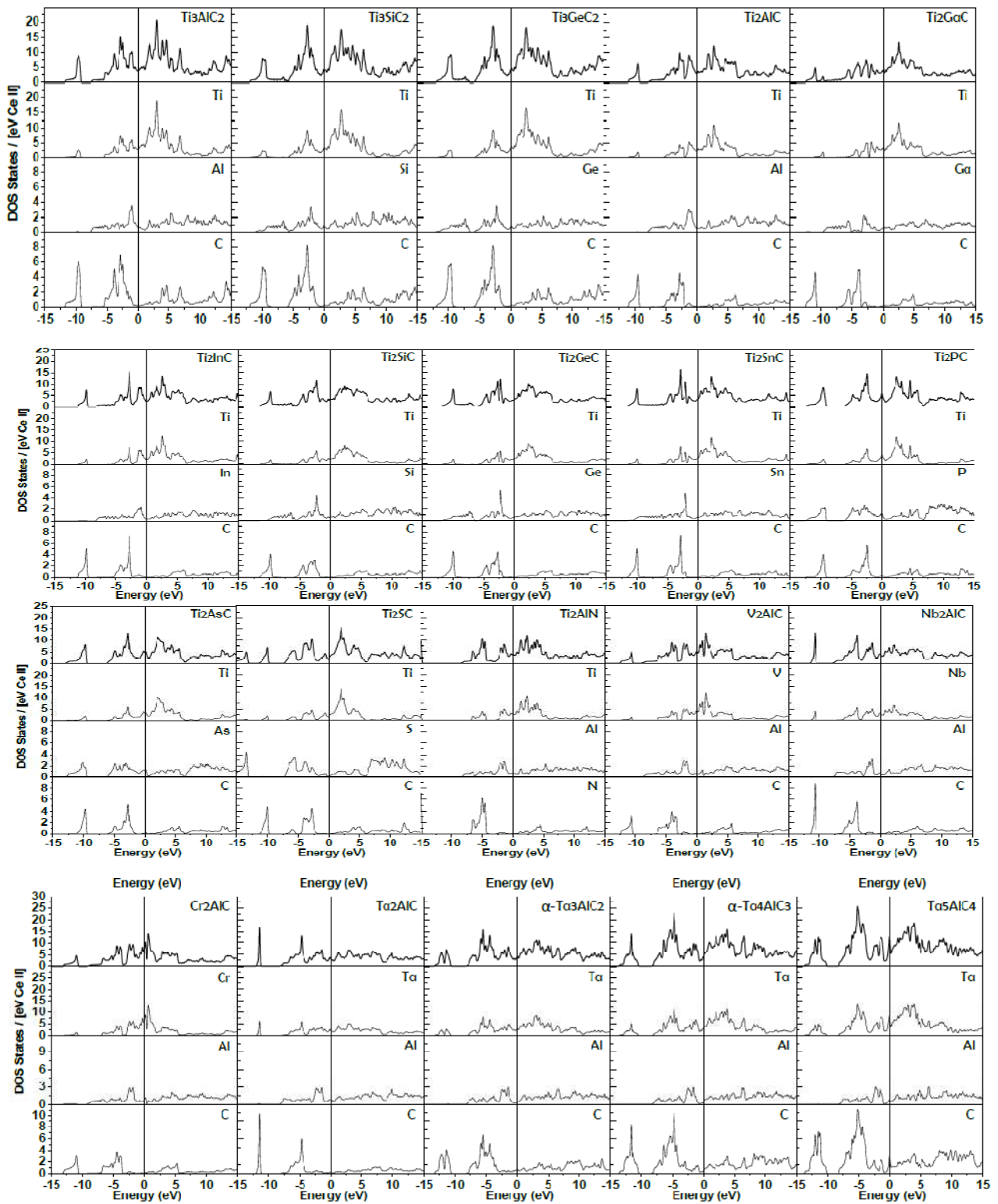


Fig. 4. Calculated DOS and atom-resolved PDOS of 20 MAX phase compounds.

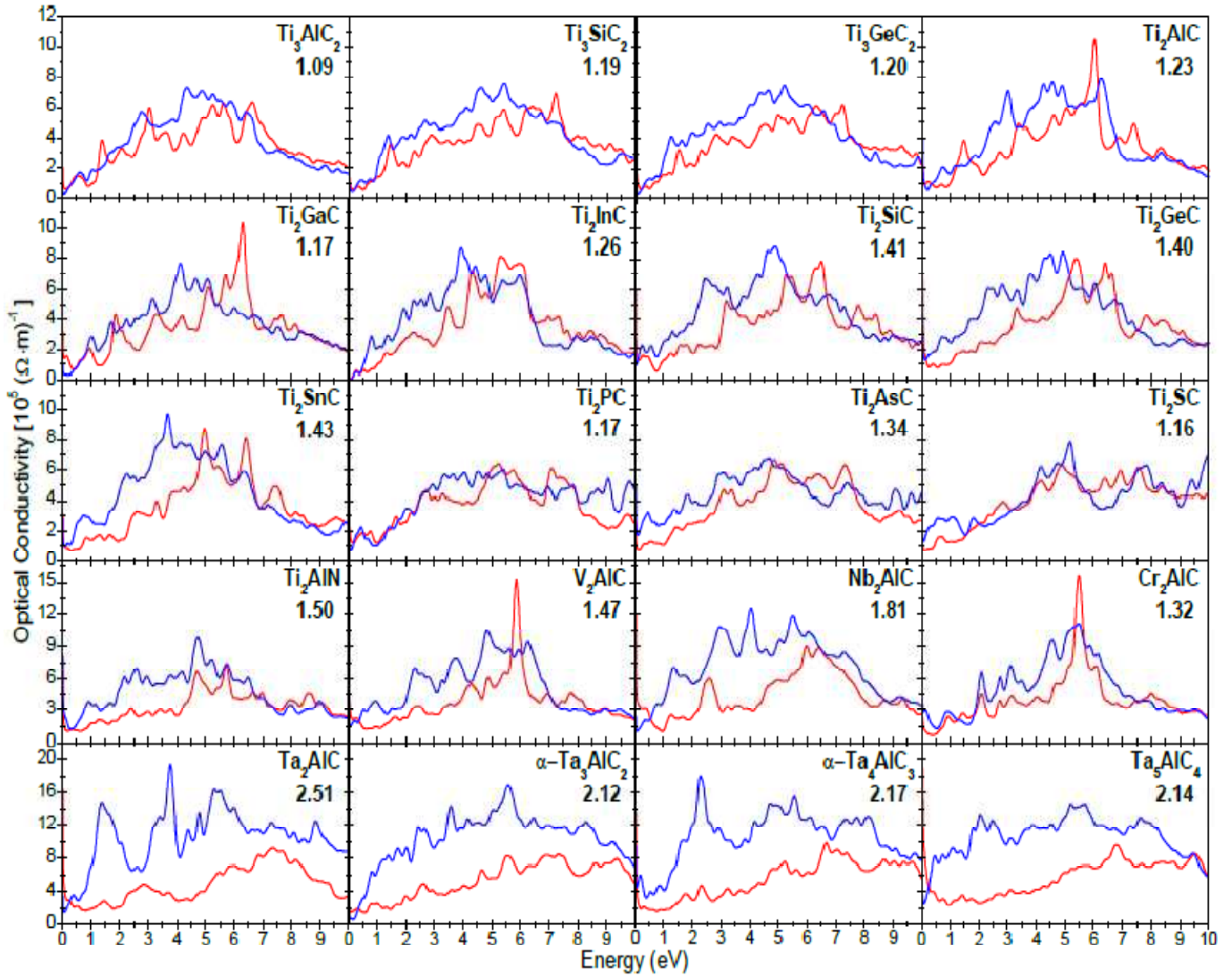


Fig. 5. Optical conductivities of 20 MAX phase compounds. Blue (red) curve show the planer (axial direction).

4. Comparative Study on Electronic, Optical and Mechanical Properties of MAX Phase Compounds

4.1. Electronic and Optical Properties

The electronic structure and optical conductivities of the MAX phases were calculated using the first-principles orthogonalized linear combination of atomic orbitals (OLCAO) method which is based on the local density approximation (LDA) of density functional theory [58-59]. This method has been demonstrated to be highly accurate and efficient when dealing with materials with complex structures for both crystalline [60-66] and non-crystalline systems [67-71]. Details of the electronic structure and optical conductivity of 20 MAX phase compounds were reported using OLCAO in reference [20]. In this review article we studied only some selected results. Fig. 4 shows the total density of states (TDOS) and atom-resolved partial density of states (PDOS) of the 20 MAX phases compounds.

The local feature of the total density of states (TDOS) curve around the Fermi-level (E_f) is a reasonable indicator of the intrinsic stability of a crystal. A local minimum at E_f implies higher structural stability because it signifies a barrier for electrons below the E_f ($E < 0$ eV) to move into unoccupied empty states ($E > 0$ eV); whereas a local maximum at E_f is usually a sign of structural instability. This semi-quantitative criterion works reasonably well for the results of Fig. 1. Ti_2InC , Ti_2SC , and Cr_2AlC have a local minimum at E_f , suggesting a higher level of stability. Ti_2PC , Ti_2AsC , and Ta_5AlC_4 show a peak in the TDOS at E_f . These facts correlate quite well with the observation that the first group of MAX phases are easier to synthesize whereas those in the second group are not [20]. The calculated optical conductivities in the 20 MAX phase compounds for frequency range between 0 and 10 eV are shown in Fig. 5. The spectra are resolved into two components, one is the planar (a - b plane) component and the other is the axial (c -direction) component, or $\sigma_{I, planar}$ and $\sigma_{I, axial}$ for short. The number indicated in each plot is the anisotropy ratio, or the averaged ($\sigma_{I, planar}/\sigma_{I, axial}$) ratio over all the data points.

From these plots, several interesting observations can be made [20]. Most of the MAX phases have the maximum optical conductivities around 5 eV and several phases show sharp peak structures with considerable anisotropy especially in the Ta series. The optical conductivity may be related to the electric conductivity in MAX phases if intra-band contribution at the frequency near 0.0 eV can be accounted for. It is conceivable that the anisotropy in optical conductivity in the low energy range could also imply that there may be similar trends in the electrical conductivity. The optical anisotropy in the low energy range of the calculation is quite low for the majority of the 20 phases which correlates well with the low anisotropy in the measured electrical conductivities. A notable exception is Nb₂AlC. Indeed, experiments by T. H. Scabarozzi et al. [21] showed that Nb₂AlC has a significantly larger anisotropy in its electrical conductivity than other MAX-phase compounds.

4.2. Mechanical and Elastic Properties

Elastic constants are very important material parameters. Evident and direct application of elastic constants is in the evaluation of elastic strains or energies in materials under stresses of various origins: external, internal and thermal [75]. The elastic constants can also provide information on the stability, stiffness, brittleness, ductility, and anisotropy of a material and propagation of elastic waves and normal mode oscillations. Moreover, knowledge of the values of elastic constants is crucial for a sound understanding of the mechanical properties of the relevant material. The most important parameters for estimating mechanical properties of materials are bulk modulus (B), shear modulus (G), Young's modulus (E) and Poisson's ratio (ν). In this section we have studied about these properties. Elastic deformation in crystalline solids is a fully reversible and nondissipative process. For hexagonal symmetry, there are five independent elastic constants; they are C_{11} , C_{12} , C_{13} , C_{33} , and C_{44} . To date, the nonavailability of large MAX single crystals has made it difficult to experimentally determine their elastic constants. What can be used until such measurements are available, however, are the results of *ab initio* calculations. In this article all the mechanical properties and elastic constant of MAX phases compounds are summarized and reviewed. All the properties are calculated by using density functional theory (DFT). The bulk moduli B_v and Young's moduli E_v are calculated by using equations 1 and 2. Also the shear moduli G_v and Poisson's ratio ν are calculated by using equations 3 & 4. The calculated results for these moduli are listed in table 4.

$$B_v = \frac{2}{9}(C_{11} + C_{12} + 2C_{13} + \frac{C_{33}}{2}) \quad (1)$$

$$E_v = \frac{9G_v B_v}{3B_v + G_v} \quad (2)$$

$$G_v = \frac{1}{15}(2C_{11} + C_{33} - C_{12} - 2C_{13}) + \frac{1}{5}[2C_{44} + \frac{1}{2}(C_{11} - C_{12})] \quad (3)$$

$$\nu = \frac{3B_v - 2G_v}{2(3B_v + G_v)} \quad (4)$$

The Poisson's ratio (ν) defined as the ratio of transverse strain to the longitudinal strain is used to reflect the stability of the material against shear and provides information about the nature of the bonding forces. It takes value: $-1 < \nu < 1/2$. No real material is known to have a negative value of ν . So this inequality can be replaced with $0 < \nu < 1/2$. Bigger the Poisson's ratio betters the plasticity. The calculated result of the Poisson's ratio shown in table 4 indicates that the max phase compound is of good plasticity. The $\nu = 0.25$ and $\nu = 0.5$ are the lower limit and upper limit for central forces in solids, respectively. The obtained value of Poisson's ratio of Ta₂GaN, Cr₂GeC and α -Ta₄AlC₃ are larger than the lower limit value, which indicates that the interatomic forces of those compounds are central forces. The bulk modulus is usually assumed to be a measure of resist deformation capacity upon applied pressure [76]. The larger the value of bulk modulus is, the stronger capacity of the resist deformation is. From figure 6 we can make a clear idea about the ability to resist deformation of Max phases. Similarly, the shear moduli are a measure of resist reversible deformation by shear stress [76]. The larger the value is, the stronger capacity of the resist shear deformation is. From Figure 6 we can make a clear idea about this. Furthermore, Young's modulus is defined as the ratio between stress and strain, and it also provided a measure of stiffness of the solid materials. The larger the value is, the stiffer the material is. The calculated result shows that the stiffness of β -Ta₄AlC₃ is the largest among all Max phases which we studied.

The elastic parameters as presented in Tables 4 allow us to make the following conclusions.

(i) The C_{ij} constants for all MAX phases are positive and satisfy the generalized criteria in Ref. [72] for mechanically stable crystals: $C_{44} > 0$, $C_{11} > |C_{12}|$, and $(C_{11} + C_{12}) C_{33} > 2C_{13}^2$.

(ii) Among the MAX phases, α -Ta₄AlC₃ is the phase with the largest bulk modulus (~266 GPa), while Ti₂CdC has the smallest B_v ~115.66 GPa. We have also seen that β -Ta₄AlC₃ has maximum Young's modulus (~404) GPa where Ti₂CdC and Zr₂PbC have the smallest E_v ~174 GPa.

(iii) The Young's modulus is defined as the ratio between stress and strain and is used to provide a measure of stiffness, i.e., the larger the value of E_v , the stiffer the material. In our case β -Ta₄AlC₃ > α -V₄AlC₃ > V₂PC > α -Ta₄AlC₃ > Ti₄AlN₃ > α -Nb₄AlC₃ > Cr₂AlC > Ti₃GeC₂ > Ti₄GeC₃ > Hf₂SC > Nb₂PC > Ta₄GaC₃ > V₂GaC > V₂AlC Hf₂PbC > Ti₂PbC > Zr₂PbC (see details in Table 5). The maximum and minimum shear moduli are obtained in Ti₄AlN₃ and Zr₂PbC. The ascending to descending values of bulk modulus (B_v), Young's modulus (E_v), shear modulus (G_v) and Poisson's ratio of all the MAX phases compounds are shown in details in Table 5.

(iv) Poisson's ratios for most of the MAX phases are around 0.2 (Table 4), which is lower than the 0.3 of Ti and most metals, and closer to the 0.19 of near-stoichiometric TiC. According to Pugh's criteria [73], a material should behave in a ductile manner if $G/B < 0.5$, otherwise it should be brittle. In our case, all the compounds have $G/B < 0.5$, (Table 5) therefore all the MAX phases compounds show ductile behavior.

Table 4. Summary of 50 MAX phase compounds, elastic constants C_{ij} determined from ab-initio calculations. Also the values of B_v , E_v , G_v , and ν are listed calculated using Equations 1, 2, 3 & 4 respectively.

Compounds	C_{11}	C_{12}	C_{13}	C_{33}	C_{44}	B_v	E_v	G_v	ν	Ref.
413 Phases										
Ti ₄ AlN ₃	420	73	70	380	128	182.88	359	153	0.172	36
Ti ₄ GeC ₃	381	96	95	349	148	187.00	341	143	0.195	37
α -Ta ₄ AlC ₃	437	158	197	416	165	266.00	364	143	0.272	38
β -Ta ₄ AlC ₃	509	143	156	440	147	263.11	404	162	0.244	39
Ta ₄ GaC ₃	389	84	78	323	131	175.66	332	140	0.185	40
α -V ₄ AlC ₃	435	121	105	384	168	212.88	384	160	0.199	39
α -Nb ₄ AlC ₃	413	124	135	328	161	215.77	353	144	0.227	39
312 Phases										
Ti ₃ SiC ₂	365	125	120	375	122	203.88	307	123	0.248	42
Ti ₃ GeC ₂	355	143	80	404	172	191.11	345	144	0.198	43
Ti ₃ AlC ₂	361	75	70	299	124	161.22	321	132	0.178	44
Ti ₃ SnC ₂	346	92	84	313	123	169.44	300	124	0.205	41
211 Phases										
Ti ₂ AlN	342	56	96	283	123	162.55	300	126	0.192	36
Ti ₂ AlC	301	59	55	278	113	135.33	272	117	0.164	45
Ti ₂ SnC	260	78	70	254	93	134.44	226	93	0.218	54
Ti ₂ GeC	279	99	95	283	125	157.66	257	105	0.227	48
Ti ₂ GaC	314	66	59	272	122	140.88	283	121	0.166	49
Ti ₂ SC	315	98	99	362	161	176.00	310	127	0.209	46
Ti ₂ CdC	258	68	46	205	33	115.66	174	69.6	0.249	53
Ti ₂ InC	288	62	53	248	88	128.88	241	102	0.186	53
Ti ₂ InN	229	56	106	248	92	138.00	208	83.3	0.248	54
Ti ₂ PbC	235	90	53	211	66	119.22	182	73.2	0.245	54
V ₂ AlC	346	71	106	314	151	174.66	324	136	0.190	51
V ₂ GeC	282	121	95	259	160	160.55	277	114	0.212	47
V ₂ GaC	343	67	124	312	157	180.88	326	136	0.199	49
V ₂ GaN	281	71	142	293	128	173.88	263	106	0.246	54
V ₂ AsC	334	109	157	321	170	203.88	318	128	0.240	57
V ₂ PC	376	113	168	386	204	226.22	376	154	0.222	54
Cr ₂ AlC	384	79	107	382	147	192.88	351	146	0.197	52
Cr ₂ GeC	315	99	146	354	89	196.22	249	96.7	0.288	47
Cr ₂ GaC	312	81	139	325	128	185.22	283	114	0.244	54
Mo ₂ GaC	294	98	107	289	127	166.77	257	111	0.227	54
Nb ₂ AlC	310	90	118	289	139	173.44	285	116	0.226	54
Nb ₂ GaC	309	80	138	262	126	176.88	270	108	0.246	54
Nb ₂ SnC	341	106	169	321	183	210.11	314	134	0.237	56
Nb ₂ InC	291	76	108	267	102	159.22	247	99.4	0.241	54
Nb ₂ AsC	334	104	169	331	167	209.22	317	127	0.247	57
Nb ₂ PC	369	113	171	316	170	218.22	333	134	0.245	54
Hf ₂ SC	344	116	138	369	175	204.55	336	137	0.226	50
Hf ₂ SnC	318	96	99	301	123	169.44	280	114	0.225	55
Hf ₂ SnN	240	62	103	236	92	139.11	211	84.5	0.247	54
Hf ₂ InC	284	69	65	243	91	134.33	238	98.7	0.204	57
Hf ₂ PbC	241	77	70	222	69	126.44	191	81	0.236	54
Ta ₂ AlC	334	114	130	322	148	193.11	303	122	0.239	54
Ta ₂ GaC	335	106	137	315	137	193.88	294	118	0.247	54
Ta ₂ GaN	333	187	150	364	141	222.66	277	107	0.292	54
Zr ₂ SnC	279	92	97	272	111	155.77	252	104	0.226	48
Zr ₂ SC	326	103	119	351	160	187.22	318	130	0.218	50
Zr ₂ InC	251	62	58	215	73	119.22	204	84	0.214	54
Zr ₂ InN	241	71	89	223	85	133.66	203	81.4	0.246	54
Zr ₂ PbC	219	70	67	206	68	116.88	174	71.4	0.246	54

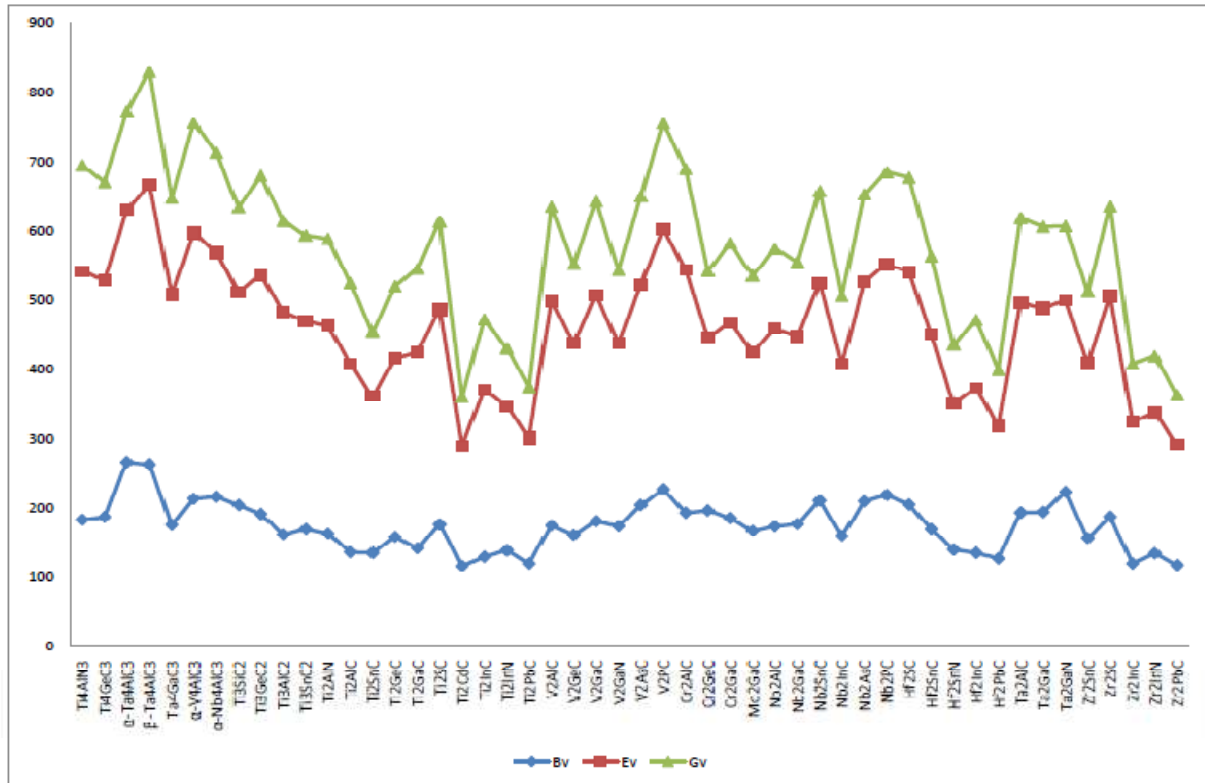


Fig. 6. Bulk moduli (B_v), shear moduli (G_v) and Young's moduli (E_v) of 50 Max Phases.

Table 5. Ascending to descending values of bulk modulus (B_v), Young's modulus (E_v), shear modulus (G_v) and Poisson's ratio of all the MAX phase compounds.

Compounds	B _v	Compounds	E _v	Compounds	G _v	Compounds	ν
α-Ta ₄ AlC ₃	266	β-Ta ₄ AlC ₃	404	β-Ta ₄ AlC ₃	162	Ta ₂ GaN	0.292
β-Ta ₄ AlC ₃	263.11	α-V ₄ AlC ₃	384	α-V ₄ AlC ₃	160	Cr ₂ GeC	0.288
V ₂ PC	226.22	V ₂ PC	376	V ₂ PC	154	α-Ta ₄ AlC ₃	0.272
Ta ₂ GaN	222.66	α-Ta ₄ AlC ₃	364	Ti ₄ AlN ₃	153	Ti ₂ CdC	0.249
Nb ₂ PC	218.22	Ti ₄ AlN ₃	359	Cr ₂ AlC	146	Ti ₃ SiC ₂	0.248
α-Nb ₄ AlC ₃	215.77	α-Nb ₄ AlC ₃	353	α-Nb ₄ AlC ₃	144	Ti ₂ InN	0.248
α-V ₄ AlC ₃	212.88	Cr ₂ AlC	351	Ti ₃ GeC ₂	144	Nb ₂ AsC	0.247
Nb ₂ SnC	210.11	Ti ₃ GeC ₂	345	Ti ₄ GeC ₃	143	Hf ₂ SnN	0.247
Nb ₂ AsC	209.22	Ti ₄ GeC ₃	341	α-Ta ₄ AlC ₃	143	Ta ₂ GaC	0.247
Hf ₂ SC	204.55	Hf ₂ SC	336	Ta ₄ GaC ₃	140	V ₂ GaN	0.246
Ti ₃ SiC ₂	203.88	Nb ₂ PC	333	Hf ₂ SC	137	Nb ₂ GaC	0.246
V ₂ AsC	203.88	Ta ₄ GaC ₃	332	V ₂ AlC	136	Zr ₂ InN	0.246
Cr ₂ GeC	196.22	V ₂ GaC	326	V ₂ GaC	136	Zr ₂ PbC	0.246
Ta ₂ GaC	193.88	V ₂ AlC	324	Nb ₂ SnC	134	Ti ₂ PbC	0.245
Ta ₂ AlC	193.11	Ti ₃ AlC ₂	321	Nb ₂ PC	134	Nb ₂ PC	0.245
Cr ₂ AlC	192.88	V ₂ AsC	318	Ti ₃ AlC ₂	132	β-Ta ₄ AlC ₃	0.244
Ti ₃ GeC ₂	191.11	Zr ₂ SC	318	Zr ₂ SC	130	Cr ₂ GaC	0.244
Zr ₂ SC	187.22	Nb ₂ AsC	317	V ₂ AsC	128	Nb ₂ InC	0.241
Ti ₄ GeC ₃	187	Nb ₂ SnC	314	Ti ₂ SC	127	V ₂ AsC	0.24
Cr ₂ GaC	185.22	Ti ₂ SC	310	Nb ₂ AsC	127	Ta ₂ AlC	0.239
Ti ₄ AlN ₃	182.88	Ti ₃ SiC ₂	307	Ti ₂ AlN	126	Nb ₂ SnC	0.237
V ₂ GaC	180.88	Ta ₂ AlC	303	Ti ₃ SnC ₂	124	Hf ₂ PbC	0.236
Nb ₂ GaC	176.88	Ti ₃ SnC ₂	300	Ti ₃ SiC ₂	123	α-Nb ₄ AlC ₃	0.227
Ti ₂ SC	176	Ti ₂ AlN	300	Ta ₂ AlC	122	Ti ₂ GeC	0.227
Ta ₄ GaC ₃	175.66	Ta ₂ GaC	294	Ti ₂ GaC	121	Mo ₂ GaC	0.227
V ₂ AlC	174.66	Nb ₂ AlC	285	Ta ₂ GaC	118	Nb ₂ AlC	0.226

Compounds	B_v	Compounds	E_v	Compounds	G_v	Compounds	ν
V ₂ GaN	173.88	Ti ₂ GaC	283	Ti ₂ AlC	117	Hf ₂ SnC	0.226
Nb ₂ AlC	173.44	Cr ₂ GaC	283	Nb ₂ AlC	116	Zr ₂ SnC	0.226
Ti ₃ SnC ₂	169.44	Hf ₂ SnC	280	V ₂ GeC	114	Hf ₂ SnC	0.225
Hf ₂ SnC	169.44	V ₂ GeC	277	Cr ₂ GaC	114	V ₂ PC	0.222
Mo ₂ GaC	166.77	Ta ₂ GaN	277	Hf ₂ SnC	114	Ti ₂ SnC	0.218
Ti ₂ AlN	162.55	Ti ₂ AlC	272	Mo ₂ GaC	111	Zr ₂ SC	0.218
Ti ₃ AlC ₂	161.22	Nb ₂ GaC	270	Nb ₂ GaC	108	Zr ₂ InC	0.214
V ₂ GeC	160.55	V ₂ GaN	263	Ta ₂ GaN	107	V ₂ GeC	0.212
Nb ₂ InC	159.22	Ti ₂ GeC	257	V ₂ GaN	106	Ti ₂ SC	0.209
Ti ₂ GeC	157.66	Mo ₂ GaC	257	Ti ₂ GeC	105	Ti ₃ SnC ₂	0.205
Zr ₂ SnC	155.77	Zr ₂ SnC	252	Zr ₂ SnC	104	Hf ₂ InC	0.204
Ti ₂ GaC	140.88	Cr ₂ GeC	249	Ti ₂ InC	102	α -V ₄ AlC ₃	0.199
Hf ₂ SnN	139.11	Nb ₂ InC	247	Nb ₂ InC	99.4	V ₂ GaC	0.199
Ti ₂ InN	138	Ti ₂ InC	241	Hf ₂ InC	98.7	Ti ₃ GeC ₂	0.198
Ti ₂ AlC	135.33	Hf ₂ InC	238	Cr ₂ GeC	96.7	Cr ₂ AlC	0.197
Ti ₂ SnC	134.44	Ti ₂ SnC	226	Ti ₂ SnC	93	Ti ₄ GeC ₃	0.195
Hf ₂ InC	134.33	Hf ₂ SnN	211	Hf ₂ SnN	84.5	Ti ₂ AlN	0.192
Zr ₂ InN	133.66	Ti ₂ InN	208	Zr ₂ InC	84	V ₂ AlC	0.19
Ti ₂ InC	128.88	Zr ₂ InC	204	Ti ₂ InN	83.3	Ti ₂ InC	0.186
Hf ₂ PbC	126.44	Zr ₂ InN	203	Zr ₂ InN	81.4	Ta ₄ GaC ₃	0.185
Ti ₂ PbC	119.22	Hf ₂ PbC	191	Hf ₂ PbC	81	Ti ₃ AlC ₂	0.178
Zr ₂ InC	119.22	Ti ₂ PbC	182	Ti ₂ PbC	73.2	Ti ₄ AlN ₃	0.172
Zr ₂ PbC	116.88	Ti ₂ CdC	174	Zr ₂ PbC	71.4	Ti ₂ GaC	0.166
Ti ₂ CdC	115.66	Zr ₂ PbC	174	Ti ₂ CdC	69.6	Ti ₂ AlC	0.164

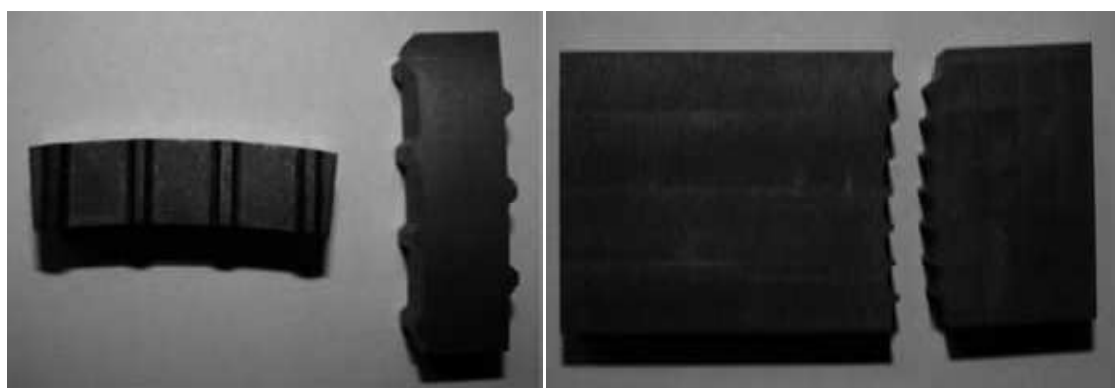
5. MAX Phase Potential Applications

The MAX phases have been proposed for numerous applications, some of which are discussed briefly below. The purpose of this section is mostly to show the rich potential for applications and the range of industries that the MAX phases could in principle impact.

5.1. Replacement for Graphite at High Temperatures

Graphite is an important high-temperature material used extensively in many industries. For example, graphite is used as connectors, heaters, furnace linings, shields, rigid

insulation, curved heating elements, and fasteners in vacuum furnaces. Graphite is also the material of choice for the hot pressing of diamond-cutting tools and other materials, for the construction industry. In general, some of the MAX phases such as Ti₂AlC have several advantages over graphite such as better wear and oxidation resistance. The ease by which Ti₂AlC can be machined to high tolerances is also an important consideration. The high strengths, moduli, and thermal conductivities of the MAX phases are also positive attributes. Figure 7 shows examples of MAX phase inserts that were actually tested in industrial dies and performed quite well.



(a)(b)

Fig. 7. (a, b) MAX-based inserts that were tested in industrial dies at elevated temperatures. (Courtesy of 3-ONE-2, LLC.)

5.2. Heating Elements

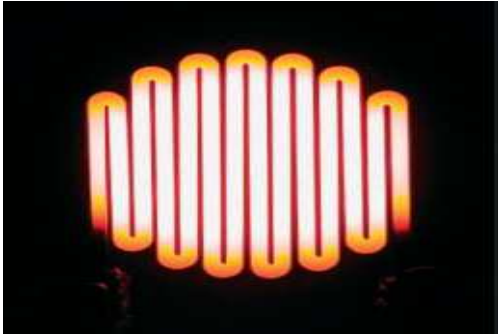


Fig. 8. Example of Ti_2AlC -based heating element resistively heated to 1450 °C in air (Courtesy of Kanthal).

In the late 1990s, Kanthal Corp. licensed the MAX technology from Drexel University. Given that one of Kanthal's core businesses is heating elements, it was not surprising that MAX phase heating elements were one of the first applications targeted by the Swedish company. The

heating element shown in figure 8 was heated up to 1350 °C and cooled down to room temperature for $\approx 10\,000$ cycles (Sundberg *et al.*, 2004). The resistance of the element was found to be very stable and the protective oxide that formed was quite adherent and protective. This heating element is quite versatile and can be used up to 1400 °C in air, argon, hydrogen, or vacuum.

5.3. High-Temperature Foil Bearings and Other Tribological Applications

A project funded by the Office of Navy Research led to the successful development of MAX based materials for foil bearings, having low friction and wear from room temperature to 823 K. Figure 9 shows a Ta_2AlC/Ag shaft and a superalloy foil after testing for 10 000 cycles in a rig. The shaft was rotated at 50 000 $rev\ min^{-1}$ [329]. Honeywell Inc. was further developing this concept.

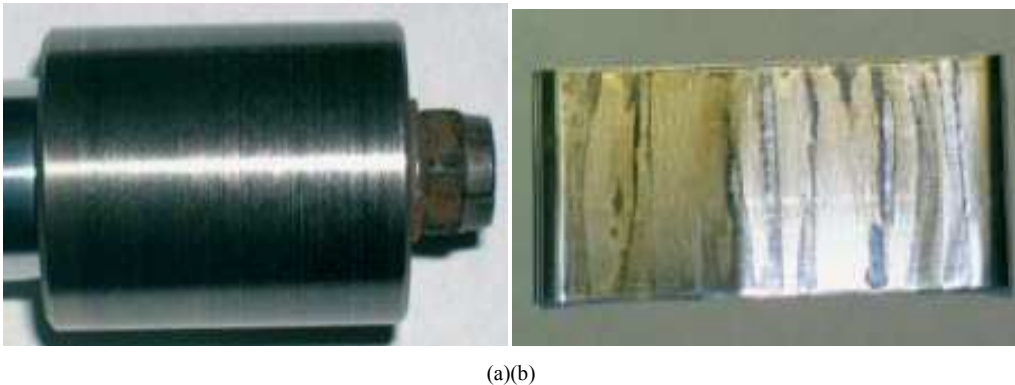


Fig. 9. (a) Ta_2AlC/Ag composite cylinder mounted on a shaft after 10000 stop-start cycles in a rig test and (b) picture of superalloy foil after rig testing [74].

5.4. Gas Burner Nozzles



Fig. 10. Pictures of Ti_2AlC and steel nozzles used in gas burners. The testing conditions that heavily corroded the steel nozzles did not appear to affect the MAX-based one.

Owing to its excellent high-temperature properties and because it forms a protective alumina layer, Ti_2AlC -based MAX phases can be used in gas burning applications where

traditional metallic alloys show limited service life (See Fig. 10). The same MAX compound can also replace metallic alloys to increase the burner process temperatures up to 1400 °C. Note that, in contrast to traditional ceramics, joining problems to existing equipment are easily overcome as MAX nozzles can be readily threaded and thus can directly replace metallic nozzles.

5.5. Tooling for Dry Drilling of Concrete

In the early 2000s, 3-ONE-2 (a small company Dr. T. El-Raghy) and Hilti developed tooling for the dry drilling of concrete, consisting of diamonds in MAX 312 (Ti_3SiC_2) segments, which were then brazed to steel. The performance of the MAX phase segments was reported to be far superior to that of current diamond/Co segments (Fig. 11 a,b). With further improvements in design to overcome the problem of smearing of concrete powders due to high temperatures and the inadequate toughness of the segments, this material may be close to market.

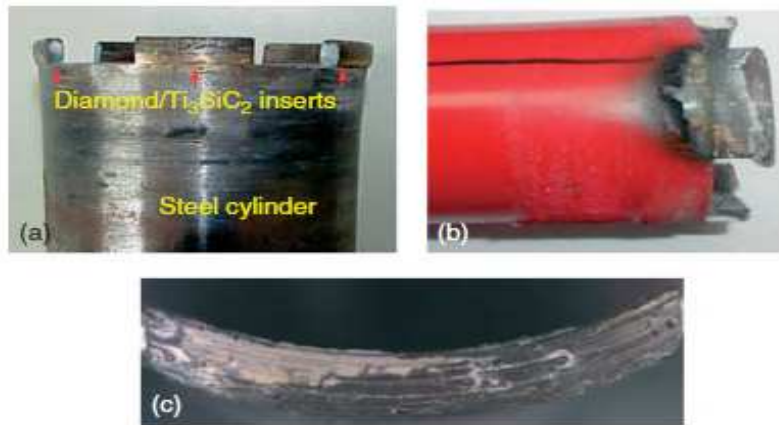


Fig. 11. Pictures of, (a) steel hollow cylinder to which diamond/Ti₃SiC₂ inserts were brazed, after dry drilling of concrete, (b) same as (a), but where the diamonds were embedded in a Co matrix; and (c) higher magnification of insert after dry drilling. (Courtesy 3-ONE-2).

5.6. Glove and Condom Formers and Nonstick Cookware

Ansell Healthcare and Drexel University signed a research agreement for developing gloves and condom formers to make latex products. The work resulted in the development of the slip casting technology for manufacturing large, thin-

walled complex parts (see Fig. 12 a–c) and a patent. In 2007, a patent was issued (El-Raghy and Lyons, 2007) for the use of the MAX phases and their coatings as durable, stick and stain and thermal shock resistant, dishwasher safe, cookware, cutlery, and other cooking utensils.

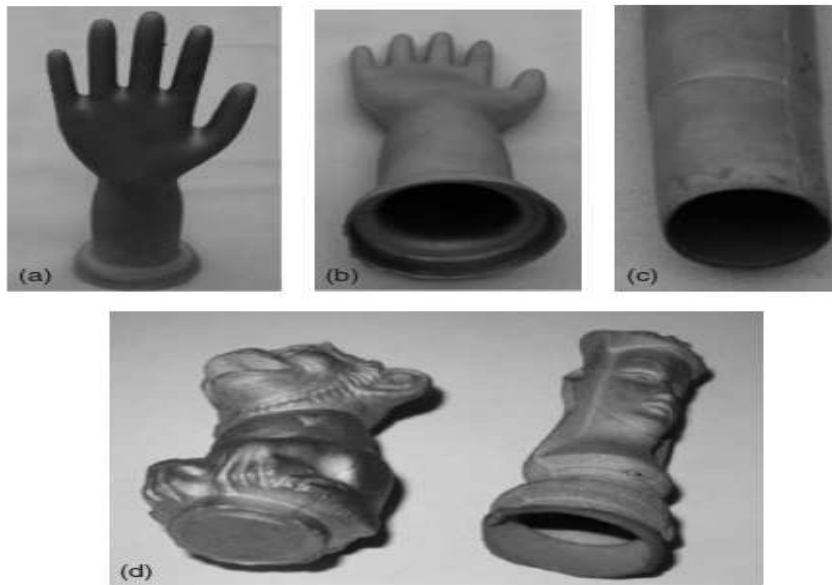


Fig. 12. Picture of (a) large, hollow, slip cast Ti₃SiC₂ glove former; (b) and (c) same as (a), but showing thin walls possible; and (d) complex solid and hollow slip cast parts starting with Maxthal powders. (Courtesy 3-ONE-2).

5.7. Application in the Nuclear Industry

There are some of the MAX phases compounds, most notably Ti₃AlC₂ and Ti₃SiC₂, are quite resistant to radiation damage (Le Flem *et al.*, 2010; Liu *et al.*, 2010; Napp'e *et al.*, 2009; Whittle *et al.*, 2010). There is also a growing body of evidence that dynamic recovery may be occurring at temperatures of 700 °C or lower. In a post-Fukushima world, it is imperative to build some accident tolerance to the Zircaloy tubes that hold the nuclear fuel. The simplest is to spray a thin coating of Ti₂AlC or Ti₃AlC₂ onto the Zircaloy

tubes. If the coatings are thin enough and are designed in such a way that in the presence of oxygen they form a thin cohesive and adhesive alumina layer, then it is possible to protect the Zircaloy tubes in the case of accident due to loss of coolant. The challenge, however, is to thermally spray the Ti₂AlC such that it does not lose its ability to form thin alumina layers. The current text on the topic shows that after high-velocity oxy-fuel, HVOF, spraying of Ti₂AlC, heating in air results in the formation of titania instead of alumina (Frodellius *et al.*, 2008; Sonestedt *et al.*, 2010a,b). The fact

that Ti_3SiC_2 does not react with molten Pb and or Pb–Bi alloys (Barnes, Dietz Rago, and Leibowitz, 2008; Heinzl, M'uller, and Weisenburger, 2009; Utili *et al.*, 2011) renders it a good material to be used for containing molten Pb or Pb–Bi alloys in nuclear reactors. In a recent paper, Sienicki *et al.* (2011) suggested that Ti_3SiC_2 could be used in an improved natural circulation Pb-cooled small modular fast reactor.

5.8. Ignition Devices and Electrical Contacts

Some of the MAX phases are used as the conductive element in spark plugs and other such ignition devices (Walker, 2010). One of the first applications for Ti_3SiC_2 was by a small Swedish company, Impact Coatings, as sputtering targets for the deposition of electrical contacts. Although the company now uses other cheaper targets, this early application is significant. Currently, others are sputter depositing Cr_2AlC thin films on steels and turbine blades (e.g. Hajas *et al.*, 2011). In some cases, MAX phase targets are used. On the basis of the growing worldwide interest in the MAX phases, it is reasonable to assume that a market for sputter targets should emerge soon. Owing to their good electrical conductivity and tribological properties, in addition to the acceptable mechanical properties, MAX phases such as Ti_3SiC_2 and Ti_3AlC_2 have been shown to perform better than carbon based pantographs for electric trains. Currently, a few leading projects are running in China, aiming for application on the high speed railway under construction.

5.9. Electrical Contact for SiC-based Devices

Presently, SiC-based devices are under development for use in electronic devices that are subjected to high temperatures and/or corrosive environments. Silicon carbide's material properties (large band-gap, high-thermal conductivity, extremely high-melting and decomposition temperatures, excellent mechanical properties, and exceptional chemical stability) are far superior to those of Si and render it suitable for operation in hostile environments. Because its band gap is nearly three times larger than that of Si, it is possible to use SiC as a semiconductor, for example, to temperatures as high as 1000 °C because of its low intrinsic carrier concentrations and operation within the dopant-controlled saturation regime required for semiconducting devices. One of the challenges of this technology is to find a material to use as an electrical contact that does not react with SiC at elevated temperatures and results in low contact resistances. In 2003, a patent was issued (Tuller, Spears, and Mlcak, 2003) for the use of Ti_3SiC_2 as an electrical contact for SiC electronic components. The major advantage of Ti_3SiC_2 is that it is in thermodynamic equilibrium with SiC. This would in turn allow the SiC devices to be operated in high-temperature environments without the contact material reacting with the SiC, and deteriorating the performance of the device. Some sensor applications are based on SiC field effect transistors that exploit the wide band gap of SiC and its chemical inertness. In such applications, there is also need a

compatible inert electrode material such as Ti_3SiC_2 .

5.10. Forming Processes and Sintering

One of the crucial advantages of working with the MAX phases is that they can be pressureless sintered to full density by heating green performs in inert atmospheres such as argon. The first report in the open literature for the pressureless sintering of a MAX phase to full density can be found in a patent that issued in 2002 (El-Raghy *et al.*, 2002). The first paper published in 2004 (Murugaiah *et al.*, 2004) not only on the pressureless sintering of Ti_3SiC_2 but also on its tape casting, a process that, not surprisingly, led to orienting the flaky prereacted hexagonal grains. In this paper, it was shown that the simplest method to producing highly oriented microstructures was to gently shake or tap the dies containing the prereacted Kanthal powders prior to sintering. The first paper published on the pressureless sintering in 2006 (Zhou *et al.*, 2006). In general, the fact that the MAX phases can be sintered to full density, without the application of pressure is an important attribute that greatly enhances their chances for commercialization. The methods for forming the green bodies are quite varied. They range from slip casting, to produce complex, thin wall shapes (e.g., Figure 11), extrusion to form tubes (Figure 9), cold pressing to form simple shapes (Figure 7) and cold isostatic pressing to metal injection molding. It is significance noting that the inherent ductility of the MAX phases help to forming green bodies without help of any binder. Spark plasma sintering (SPS) is also emerging as a viable method to fabricate and densify the MAX phases (Cui *et al.*, 2012; Hu *et al.*, 2009, 2011b; Zhang *et al.*, 2003). Currently there is little work, however, comparing the high-temperature properties of samples made by SPS with those made by reactive hot pressing or pressureless sintered commercial powders.

In addition to the applications mentioned above, a number of other potential applications have been found. These include: electrodes, exhaust gas filters for automobiles, free-cutting elements, microelectronics, biomaterials, damping materials (high stiffness and up to high temperatures), corrosion resistant materials, surface coatings, defense applications, such as armor, nuclear applications, low dimensional materials, and substrates for CVD diamond.

6. Conclusion

The MAX phases have attracted considerable attention and are garnering new devotees because they have a quite unusual combination of properties. The fact that their chemistries can be altered while keeping the structure the same allows for relatively rapid understanding. The emergence of possibly magnetic MAX phases is an exciting development that would greatly enhance their potential applications. On the mechanical side, the fact that dislocations are confined to 2D is proving invaluable in elucidating the deformation behavior of layered solids in general, and ones that are also conductive in particular. The most urgent issue in MAX phase research is to develop

viable commercial applications for these materials. With the preliminary and potential application fields discussed above, market penetration by MAX phase materials will create more stimuli to carry out more research and development on this family of layered metallic ceramics. Research on MAX phases is currently funded by agencies, science foundations and defense industries in the USA, China, Europe and Australia. However, funding for research on MAX phases from governmental agencies in Japan is almost zero. The likelihood of the Japanese government funding such research remains small until a clear market scenario is available.

Another important issue is the search for new MAX phases. First, to better understand the MAX phases themselves, both those known to exist and those theoretically predicted to be thermodynamically and mechanically stable. To do so, thorough experimental investigations into the properties are needed. The second priority is to discover more MAX phases. It is encouraging that in the past few years many MAX phases, particularly 413 and 312 phases, have been discovered. More 312 or 211 MAX phases, plus their solid solutions, which are numerous, are awaiting exploration. In this review paper we have studied most of the MAX phase compounds, their different properties and applications in different sectors. We hope that the researches described in this overview will be helpful for the discovery of new MAX phase compound and their practical and possible applications in modern technology in near future.

References

- [1] M. W. Barsoum: Prog. Solid State Chem., 2000, 28, 201–281.
- [2] Z. M. Sun, H. Hashimoto, Z. F. Zhang, S. L. Yang and S. Tada: Mater. Trans., 2006, 47, 170–174.
- [3] W. Jeitschko, H. Nowotny, and F. Benesovsky, Monatsh. Chem., 94, 672 (1963).
- [4] W. Jeitschko, H. Nowotny, and F. Benesovsky, Monatsh. Chem., 94, 844 (1963).
- [5] W. Jeitschko, H. Nowotny, and F. Benesovsky, Monatsh. Chem., 94, 1198 (1964).
- [6] W. Jeitschko, H. Nowotny, and F. Benesovsky, Monatsh. Chem., 95, 178 (1964).
- [7] W. Jeitschko, H. Nowotny, and F. Benesovsky, Monatsh. Chem., 95, 1004 (1964).
- [8] M. W. Barsoum, Prog. Solid State Chem., 28, 201 (2000).
- [9] H. B. Zhang, Y. W. Bao, and Y. C. Zhou, J. Mater. Sci. Technol., 25, 1 (2009).
- [10] J. Y. Wang and Y. C. Zhou, Annual Rev. Mater. Res., 39, 415 (2009).
- [11] P. Eklund, M. Beckers, U. Jansson, et al., Thin Solid Films, 518, 1851 (2010).
- [12] J. P. Palmquist, S. Li, P. O. Persson, et al., Phys. Rev., B70, 165401 (2004).
- [13] H. Hogberg, P. Eklund, J. Emmerlich, et al., J. Mater. Res., 20, 779 (2005).
- [14] S. E. Lofland, J. D. Hettinger, T. Meehan, et al., Phys. Rev., B74, 174501 (2006).
- [15] A. D. Bortolozzo, Z. Fisk, O. H. Sant'Anna, et al., Physica, C469, 256 (2009).
- [16] Barsoum, M.W., Brodtkin, D., & El-Raghy, T., Layered Machinable Ceramics, For High Temperature Applications. Scrip. Met. et. Mater. 36, 535-541 (1997)
- [17] Nowotny, H., Strukturchemie Einiger Verbindungen der Übergangsmetalle mit den elementen C, Si, Ge, Sn. Prog. Solid State Chem. 2, 27 (1970)
- [18] Barsoum, M.W. & El-Raghy, T., Synthesis and Characterization of a Remarkable Ceramic: Ti₃SiC₂. J. Amer. Cer. Soc. 79 (7), 1953-1956 (1996)
- [19] Barsoum, M.W. & El-Raghy, T., Synthesis and Characterization of a Remarkable Ceramic: Ti₃SiC₂. J. Amer. Cer. Soc. 79 (7), 1953-1956 (1996)
- [20] Yuxiang Mo, Paul Rulis, and W.Y. Ching, Yuxiang Mo, Paul Rulis, W.Y. Ching, Electronic structure and Optical properties of 20 MAX phase compounds, submitted to Phys. Rev. B. (2012).
- [21] T. H. Scabarozzi, J. Roche, A. Rosenfeld, S. H. Lim, L. Salamanca-Riba, I. Takeuchi, M. W. Barsoum, J. D. Hettinger, S. E. Lofland, Synthesis and Characterization of Nb₂AlC Thin Films, Thin Solid Films, 517, 2920-2933 (2009).
- [22] C. M. Fang, R. Ahuja and O. Eriksson: J. Appl. Phys., 2007, 101, 013511.
- [23] G. Hug: Phys. Rev. B, 2006, 74B, 184113.
- [24] D. Music, Z. M. Sun and J. M. Schneider: Solid State Commun., 2005, 133, 381–383.
- [25] S. Dubois, T. Cabioc'h, P. Chartier, V. Gauthier and M. Jaouen: J. Am. Ceram. Soc., 2007, 90, 2642- 2644.
- [26] M. B. Kanoun and M. Jaouen: J. Phys.-Cond. Matter, 2008, 20, 085211.
- [27] J. Etzkorn, M. Ade and H. Hillebrecht: Inorg. Chem., 2007, 46, 1410–1418.
- [28] Y. C. Zhou, F. L. Meng and J. Zhang: J. Am. Ceram. Soc., 2008, 91, 1357–1360.
- [29] A. Grechnev, S. Li, R. Ahuja, O. Eriksson, U. Jansson and O. Wilhelmsson: Appl. Phys. Lett., 2004, 85, 3071–3073.
- [30] H. Hogberg, P. Eklund, J. Emmerlich, J. Birch and L. Hultman: J. Mater. Res., 2005, 20, 779–782.
- [31] C. F. Hu, Z. J. Lin, L. F. He, Y.W. Bao, J. Y. Wang, M. S. Li and Y. C. Zhou: J. Am. Ceram. Soc., 2007, 90, 2542–2548.
- [32] C. F. Hu, F. Z. Li, L. F. He, M. Y. Liu, J. Zhang, J. M. Wang, Y. W. Bao, J. Y. Wang and Y. C. Zhou: J. Am. Ceram. Soc., 2008, 91, 2258–2263.
- [33] M. W. Barsoum, J. Golczewski, H. J. Seifert and F. Aldinger: J. Alloys Compd, 2002, 340, 173–179.
- [34] T. El-Raghy, S. Chakraborty and M. W. Barsoum: J. Eur. Ceram. Soc., 2000, 20, 2619–2625.

- [35] W. B. Tian, P. L. Wang, G. J. Zhang, Y. M. Kan, Y. X. Li and D. S. Yan: *Scr. Mater.*, 2006, 54, 841–846.
- [36] Holm, B., Ahuja, R., Li, S., and Johansson, B. (2002) Theory of ternary layered system Ti-Al-N. *J. Appl. Phys.*, 91, 9874–9877.
- [37] Li, C.-W. and Wang, Z. (2010) First-principles study of structural, electronic, and mechanical properties of the nanolaminate compound Ti_4GeC_3 under pressure. *J. Appl. Phys.*, 107, 123511.
- [38] Du, Y.L., Sun, Z.M., Hashimoto, H., and Tian, W.B. (2008a) Elastic properties of Ta_4AlC_3 studied by first-principles calculations. *Solid State Commun.*, 147, 246–249.
- [39] Wang, J., Zhou, Y., Lin, Z., and Hu, J. (2008) Ab initio study of polymorphism in layered ternary carbide M_4AlC_3 ($M = V, Nb$ and Ta). *Scr. Mater.*, 58, 1043–1046.
- [40] He, X., Bai, Y., Zhu, C., and Barsoum, M.W. (2011) Polymorphism of newly-discovered Ti_4GaC_3 : a first-principle study. *Acta Mater.*, 59, 5523–5533.
- [41] He, X., Bai, Y., Zhu, C., Sun, Y., Li, M., and Barsoum, M.W. (2010) General trends in the structural, electronic and elastic properties of the M_3AlC_2 phases ($M =$ transition metal): a first-principle study. *Comput. Mater. Sci.*, 49, 691–698.
- [42] Holm, B., Ahuja, R., and Johansson, B. (2001) Ab initio calculations of the mechanical properties of Ti_3SiC_2 . *Appl. Phys. Lett.*, 79, 1450.
- [43] Finkel, P., Seaman, B., Harrell, K., Hettinger, J.D., Lofland, S.E., Ganguly, A., Barsoum, M.W., Sun, Z., Li, S., and Ahuja, R. (2004) Low temperature elastic, electronic and transport properties of $Ti_3Si_{1-x}GexC_2$ solid solutions. *Phys. Rev. B*, 70, 085104.
- [44] Sun, Z., Li, S., Ahuja, R., and Schneider, J.M. (2004) Calculated elastic properties of M_2AlC ($M = Ti, V, Cr, Nb$ and Ta). *Solid State Commun.*, 129, 589–592.
- [45] Du, Y.L., Sun, Z.-M., Hashimoto, H., and Barsoum, M.W. (2009a) Theoretical investigations on the elastic and thermodynamic properties of $Ti_2AlC_{0.5}N_{0.5}$ solid solution. *Phys. Lett. A*, 374, 78–82.
- [46] Du, Y.L., Sun, Z.M., Hashimoto, H., and Tian, W.B. (2008b) First-principles study on electronic structure and elastic properties of Ti_2SC . *Phys. Lett. A*, 372, 5220–5223.
- [47] Bouhemadou, A. (2009a) Calculated structural, electronic and elastic properties of M_2GeC ($M = Ti, V, Cr, Zr, Nb, Mo, Hf, Ta$ and W). *Appl. Phys. A*, 96, 959–967.
- [48] Bouhemadou, A. (2008b) Prediction study of structural and elastic properties under pressure effect of M_2SnC ($M = Ti, Zr, Nb, Hf$). *Physica B-Condens. Matter*, 403, 2707.
- [49] Bouhemadou, A. and Khenata, R. (2007) Prediction study of structural and elastic properties under the pressure effect of M_2GaC , $M = Ti, V, Nb, Ta$. *J. Appl. Phys.*, 102, 043528.
- [50] Bouhemadou, A. and Khenata, R. (2008) Structural, electronic and elastic properties of M_2SC ($M = Ti, Zr, Hf$) compounds. *Phys. Lett. A*, 372, 6448–6452.
- [51] Wang, J. and Zhou, Y. (2004a) Dependence of elastic stiffness on electronic band structure of nanolaminate M_2AlC ($M = Ti, V, Nb$ and Cr) ceramics. *Phys. Rev. B*, 69, 214111.
- [52] Sun, Z., Li, S., Ahuja, R., and Schneider, J.M. (2004) Calculated elastic properties of M_2AlC ($M = Ti, V, Cr, Nb$ and Ta). *Solid State Commun.*, 129, 589–592.
- [53] Bai, Y., He, X., Li, M., Sun, Y., Zhu, C., and Li, Y. (2010) Ab initio study of the bonding and elastic properties of Ti_2CdC . *Solid State Sci.*, 12, 144–147.
- [54] Cover, M.F., Warschkow, O., Bilek, M.M., and McKenzie, D.R. (2009) A comprehensive survey of M_2AX phase elastic properties. *J. Phys.: Condens. Matter*, 21, 305403.
- [55] Kanoun, M.B., Goumri-Said, S., and Reshak, A.H. (2009b) Theoretical study of mechanical, electronic, chemical bonding and optical properties of $Ti_2SnC, Zr_2SnC, Hf_2SnC$ and Nb_2SnC . *Comput. Mater. Sci.*, 47, 491–500.
- [56] Kanoun, M.B., Goumri-Said, S., and Jaouen, M. (2009a) Steric effect on the M site of nanolaminate compounds M_2SnC ($M = Ti, Zr, Hf$ and Nb). *J. Phys.: Condens. Matter*, 21, 045404–045406.
- [57] Scabarozzi, T.H., Amini, S., Leffer, O., Ganguly, A., Gupta, S., Tambussi, W., Clipper, S., Spanier, J.E., Barsoum, M.W., Hettinger, J.D. *et al.* (2009) Thermal expansion of select MAX phases measured by high temperature X-ray diffraction and dilatometry. *J. Appl. Phys.*, 105, 013543.
- [58] P. Hohenberg and W. Kohn, *Phys. Rev.* 136, B864 (1964).
- [59] W. Kohn and L. J. Sham, *Phys. Rev. A* 140, 1133 (1965).
- [60] W. Y. Ching and P. Rulis, *Phys. Rev. B* 73, 045202 (2006).
- [61] W. Y. Ching, L. Ouyang, P. Rulis, and H. Yao, *Phys. Rev. B* 78, 014106 (2008).
- [62] W. Y. Ching and P. Rulis, *Phys. Rev. B* 77, 035125 (2008).
- [63] L. Liang, P. Rulis, B. Kahr, and W. Y. Ching, *Phys. Rev. B* 80, 235132 (2009).
- [64] S. Aryal, P. Rulis, and W. Y. Ching, *Am. Mineral.* 93, 114 (2008).
- [65] L. Liang, P. Rulis, and W. Y. Ching, *Acta Biomater.* 6, 3763 (2010).
- [66] W. Y. Ching, S. Aryal, P. Rulis, and W. Schnick, *Phys. Rev. B* 83, 155109 (2011).
- [67] P. Rulis and W. Ching, *J. Mater. Sci.* 46, 4191 (2011).
- [68] P. Rulis, H. Yao, L. Ouyang, and W. Y. Ching, *Phys. Rev. B* 76, 245410 (2007).
- [69] W. Y. Ching, P. Rulis, L. Ouyang, and A. Misra, *Appl. Phys. Lett.* 94, 051907 (2009).
- [70] W. Y. Ching, P. Rulis, L. Ouyang, S. Aryal, and A. Misra, *Phys. Rev. B* 81, 214120 (2010).
- [71] L. Liang, P. Rulis, L. Ouyang, and W. Y. Ching, *Phys. Rev. B* 83, 024201 (2011).
- [72] M. Born and K. Huang, *Dynamical Theory of Crystal Lattices* (Clarendon, Oxford, 1956).
- [73] E. I. Isaev, S. I. Simak, I. A. Abrikosov, R. Ahuja, Y. K. Vekilov, M. I. Katsnelson, A. I. Lichtenstein, and B. Johansson, *J. Appl. Phys.* 101, 123519 (2007).

- [74] S. Gupta, D. Filimonov, T. Palanisamy, T. El-Raghy and M. W. Barsoum: *Wear*, 2007, 262, 1479–1489.
- [75] K. Tanaka, M. Koiwa, *Intermetallics* 4 (1996) S29eS39.
- [76] S.F. Pugh, *Philos. Mag.* 45 (1954) 823.